© 2017. Published by The Company of Biologists Ltd | Journal of Cell Science (2017) 130, 3685-3697 doi:10.1242/jcs.205427

RESEARCH ARTICLE

The DUX4 homeodomains mediate inhibition of myogenesis and are functionally exchangeable with the Pax7 homeodomain

Darko Bosnakovski[1,2], Erik A. Toso[2], Lynn M. Hartweck[2], Alessandro Magli[3], Heather A. Lee[2], Eliza R. Thompson[2], Abhijit Dandapat[2], Rita C. R. Perlingeiro[3] and Michael Kyba[2,*]

ABSTRACT

Facioscapulohumeral muscular dystrophy (FSHD) is caused by inappropriate expression of the double homeodomain protein DUX4. DUX4 has bimodal effects, inhibiting myogenic differentiation and blocking MyoD at low levels of expression, and killing myoblasts at high levels. Pax3 and Pax7, which contain related homeodomains, antagonize the cell death phenotype of DUX4 in C2C12 cells, suggesting some type of competitive interaction. Here, we show that the effects of DUX4 on differentiation and MyoD expression require the homeodomains but do not require the C-terminal activation domain of DUX4. We tested the set of equally related homeodomain proteins (Pax6, Pitx2c, OTX1, Rax, Hesx1, MIXL1 and Tbx1) and found that only Pax3 and Pax7 display phenotypic competition. Domain analysis on Pax3 revealed that the Pax3 homeodomain is necessary for phenotypic competition, but is not sufficient, as competition also requires the paired and transcriptional activation domains of Pax3. Remarkably, substitution mutants in which DUX4 homeodomains are replaced by Pax7 homeodomains retain the ability to inhibit differentiation and to induce cytotoxicity.

KEY WORDS: Facioscapulohumeral muscular dystrophy, DUX4, Myogenesis, Homeodomain, Pax3, Pax7

INTRODUCTION

Facioscapulohumeral muscular dystrophy (FSHD) is a dominant inherited myopathy caused by mutations that lead to loss of repeat-induced silencing of the D4Z4 repeat array on chromosome 4 (Gabellini et al., 2002; Lemmers et al., 2012; van Overveld et al., 2003; Wijmenga et al., 1992). This in turn provides favorable conditions for expression of *DUX4*, a gene embedded within each D4Z4 repeat unit (Gabriëls et al., 1999). In several independent studies, *DUX4* mRNA or protein was detected at extremely low levels, specifically in myoblasts from FSHD patients (Block et al., 2013; Dixit et al., 2007; Jones et al., 2012; Kowaljow et al., 2007; Snider et al., 2010). DUX4 (double homeobox protein 4) functions as a transcriptional activator, inducing expression of hundreds of target genes (Bosnakovski et al., 2008b; Geng et al., 2012) through a mechanism involving p300/CBP (Choi et al., 2016).

Cultured myoblasts from FSHD patients exhibit greater sensitivity to oxidative stress and show reduced levels of expression of MyoD and downstream target genes, compared with controls (Celegato et al., 2006; Krom et al., 2012; Rahimov et al., 2012; Tassin et al., 2012; Tsumagari et al., 2011; Winokur et al., 2003a,b). In our previous work, we demonstrated that *DUX4*, when expressed at low levels in C2C12 myoblasts, recapitulates aspects of this FSHD myoblast phenotype, namely that it sensitizes cells to oxidative stress and severely reduces *MyoD* mRNA and protein levels (Bosnakovski et al., 2008b). High levels of *DUX4* expression caused cell death (Bosnakovski et al., 2008b). In addition to these effects, myoblasts expressing low levels of *DUX4* had diminished differentiation potential, presumably caused by dysregulation of myogenic regulatory factors (MRFs), including MyoD (Bosnakovski et al., 2008b). The transcriptional profile of DUX4 has been described as characteristic of a less differentiated state (Knopp et al., 2016). Similar assays performed on *DUX4c* showed that its expression also downregulated MyoD and inhibited myogenic differentiation, but was not cytotoxic (Bosnakovski et al., 2008a). *DUX4c* is encoded by a satellite repeat 42 kb centromeric to the D4Z4 repeat array and it lacks the 82 C-terminal amino acids of DUX4 because of a frameshift, suggesting that the C-terminus is not necessary for effects on myogenesis.

The N-terminus of DUX4 contains its only highly conserved and recognizable domains, two paired-class homeodomains. Both homeodomains bear significant similarity to the homeodomains of PAX3 and PAX7, the paired-class homeodomain proteins that act at the apex of the myogenic regulatory hierarchy and are expressed in adult satellite cells (Buckingham et al., 2003; Montarras et al., 2005; Seale et al., 2000). We hypothesized that DUX4 might impair myogenesis, and therefore muscle regeneration in FSHD, through interference with PAX3 and/or PAX7 or through misregulation of their homeodomain-dependent target genes in satellite cells or their activated progeny. Consistent with the idea that DUX4 and Pax3/Pax7 can compete with one another, perhaps for regulation of crucial target genes, both *Pax3* and *Pax7* acted as dose-dependent suppressors of *DUX4*-induced cytotoxicity when overexpressed in C2C12 cells (Bosnakovski et al., 2008b). However, although the homeodomains of Pax3 and Pax7 are highly related to those of DUX4, a number of other non-myogenic proteins have homeodomains of equal or greater similarity, including Pax6, OTX1, Rax, Hesx and MIXL1. It is unclear whether the competition between DUX4 and Pax3/Pax7 is a result of competition between their homeodomains and, if so, whether this is a generic feature of the paired class of homeodomains rather than a specific feature of certain members. Furthermore, it is not known whether proteins with homeodomains of greater similarity than Pax3 and Pax7 compete more effectively with DUX4. In this study, we investigate the homeodomains of DUX4 and their competitive interactions with other homeodomain-containing proteins using the techniques of co-overexpression, domain analysis and homeodomain substitution. The results point to a unique relationship between the homeodomains of DUX4 and those of Pax3 and Pax7.

[1]Faculty of Medical Sciences, University Goce Delcev-Stip, 2000 Stip, R. Macedonia. [2]Lillehei Heart Institute, Department of Pediatrics, University of Minnesota, Minneapolis, MN 55014, USA. [3]Lillehei Heart Institute, Department of Medicine, University of Minnesota, Minneapolis, MN 55104, USA.

*Author for correspondence (kyba@umn.edu)

A.D., 0000-0003-2692-4386; R.C.R.P., 0000-0001-9412-1118; M.K., 0000-0002-5579-7534

Received 24 April 2017; Accepted 11 September 2017

Journal of Cell Science

Journal of Cell Science (2017) 130, 3685-3697 doi:10.1242/jcs.205427

RESULTS

Generation of inducible myoblasts bearing DUX4 deletions

We previously showed that DUX4 expressed at high levels in different cell types induces rapid cell death and, at low levels, interferes with master myogenic transcription factors MyoD and Myf5, strongly inhibiting myogenesis. To investigate which domains within DUX4 are necessary for induction of these phenotypes, we made a series of deletion constructs and generated doxycycline-inducible mouse C2C12 myoblast cell lines by inducible cassette exchange (ICE) (Bosnakovski et al., 2008b). As a template for these deletion constructs, we began with a DUX4 construct derived from the terminal D4Z4 repeat of a 4qA161 allele (Gabriëls et al., 1999), which contained the 3′UTR sequence up to the *EcoRI* site (Fig. 1A). We wished to determine the roles of the N-terminus (the homeodomains) and C-terminus (missing in DUX4c), and whether D4Z4 RNA or some additional elements from the 3′UTR play a role in the DUX4 phenotypes described above. To explore the requirement for homeodomains 1 and 2 (HD1 and HD2), we made a construct initiating precisely at homeodomain 2 [ΔHD1(81–424); amino acids are listed in parentheses] and a construct initiating where HD2 ends, that is, lacking both homeodomains [ΔHD(1+2)(157–424)]; an ATG was added to start translation. To analyze the role of the C-terminus, a deletion series was made (Fig. 1A). To evaluate activity of the RNA, or some additional unknown product that might be transcribed from the D4Z4 sequence, we (1) made constructs in which we deleted the ATG (ΔATG) of DUX4, (2) created a sequence that initiated at an internal *Bsu 36I* site (Δ5′+3′UTR) and (3) deleted the entire internal sequence between the first and last *Pvu II* sites [ATG(1–75)+Δ3′UTR] (Fig. 1A). The possibility of an activity being encoded by the antisense strand was tested by placing the D4Z4 sequence in reverse orientation with respect to the inducible promoter (DUX4-opp, Fig. 1A). All constructs were integrated into the unique ICE locus in iC2C12 cells by ICE recombination; inducible cell lines resistant to G418 were generated as previously described (Bosnakovski et al., 2008b). Each construct was expressed from the same locus and could be regulated in a dose-responsive manner with doxycycline. RNA for all constructs was detected by the reverse transcription polymerase chain reaction (RT-PCR). Proteins for each construct were evaluated by western blot using antibodies that recognize N-terminal (P2G4), central (9A12) or C-terminal (E5-5) epitopes of DUX4 (Fig. 1B) (Dixit et al., 2007; Geng et al., 2011). Using the 9A12 antibody, we were able to detect all the deletion proteins except DUX4(1–217), DUX4(1–75)+Δ3′UTR and Δ5′+3′UTR. The DUX4(1–217) deletion, but not ΔDUX4(1–75)+Δ3′UTR or Δ5′+3′UTR, was recognized by P2G4. By combining the 9A12 and P2G4 antibodies we could evaluate the relative sizes of all constructs for which antibodies exist; these were as expected and ranged from ∼30 kDa [DUX4(1–217)] to ∼51 kDa (DUX4+3′ UTR). Notably, the protein levels of all constructs lacking the C-terminus [DUX4c, DUX4(1–377) and DUX4(1–399)] were increased relative to those having a full C-terminus (Fig. 1B). Interestingly, in using the 9A12 antibody to detect the construct in which the start codon was removed (ΔATG), we saw a smaller band of approximately 40 kDa, suggesting the presence of a cryptic internal translation initiation site (Fig. 1B). This protein is probably initiated from an internal leucine (as described by Snider et al., 2010), is apparently inactive and resembles the homodomain deletions. To confirm that deletion constructs were homogenously inducible in all cells of the generated cell lines, we performed immunostaining after 20 h doxycycline induction (Fig. 1C).

Both homeodomains and C-terminus are necessary for cytotoxicity

We assayed all of the deletion cell lines for cell viability by plating cells at equal density (2000 cells/well in 96-well plates), inducing the following day with various doses of doxycycline, and quantifying viability at 48 h post-induction. Cell death was observed at 24 h only in cell lines expressing full-length DUX4 constructs [i.e. DUX4(1–424) and DUX4+3′UTR]; the same effect was evident at 48 and 72 h post-induction (data not shown). However, in the construct with the smallest 3′ deletion [DUX4(1–399)], we observed decreased confluency but obvious cell death by visual inspection (Fig. 2A). Measurement of ATP content confirmed the morphologically observed cell death induced by full-length DUX4 (Fig. 2B). In addition, DUX4(1–399)-expressing cells showed significantly decreased cell viability (Fig. 2B). On the other hand, ATP content in other cell lines was similar, regardless of the levels and duration of expression (Fig. 2B). This experiment clearly shows that, in addition to the N-terminal homeodomains, the C-terminus of DUX4 is necessary for toxicity, as previously described (Bosnakovski et al., 2008a). To clarify the effect of DUX4(1–399), which contains the smallest C-terminal deletion, we analyzed the levels of apoptosis and proliferation in induced cells and found a 1.6-fold increase in apoptotic cells in cultures that expressed DUX4(1–399) for 18 h (Fig. 2C,D). This construct also affected the proliferation rate, as indicated by a 30% decreased incorporation of 5-ethynyl-2′-deoxyuridine (EdU) compared with control uninduced cells (Fig. 2E,F). The other constructs, which showed no effect on ATP content, did not induce apoptosis or affect cell cycle (Fig. 2C–F).

The homeodomains alone are sufficient to alter MRF expression and to block differentiation

DUX4 and DUX4c, which lacks the C-terminus, both interfere with myogenic regulators, predominantly with MyoD and its downstream targets (Bosnakovski et al., 2008a,b). We previously reported that DUX4 and DUX4c rapidly suppress MyoD within 2 h of induction, even at low doses. To identify domains essential for this phenotype, we induced DUX4 constructs in proliferating cells and analyzed the expression levels of MyoD and Myf5 by RT-qPCR. After a short 6 h induction, we found that every construct retaining both homeodomains (like DUX4 and DUX4c) provoked a reduction in MyoD (Fig. 3A). However, for Myf5, the constructs bearing larger C-terminal deletions [DUX4(1–217)] downregulated Myf5 expression (like DUX4c), whereas the shortest C-terminal deletion [DUX4(1–399)] moderately increased Myf5, similarly to wild-type (WT) DUX4 (Fig. 2A). Constructs with N-terminal deletions had no influence on MyoD or Myf5 (not shown).

To test the functional relevance of interactions between deletion constructs and myogenic regulators, we induced myogenic differentiation and analyzed the levels of myotube formation. All of the cell lines were cultured to 80% confluence in proliferation medium, at which point they were differentiated with myogenic differentiation medium containing horse serum and insulin and then induced with doxycycline at low (25 ng ml^{-1}) and high doses (250 ng ml^{-1}). Formation of terminally differentiated, multinucleated myotubes was evaluated by staining for myosin heavy chain (MHC) and calculating the myotube fusion index. Consistent with their ability to repress MyoD, only those constructs that contained intact homeodomains inhibited myogenic differentiation. Only sporadic MHC-positive cells were found in the induced cells, compared to the robust differentiation observed in uninduced cells (Fig. 3B–D). Interestingly, the effect on differentiation was partially dependent on the amount of C-terminus remaining. At the low doxycycline level

Journal of Cell Science (2017) 130, 3685-3697 doi:10.1242/jcs.205427

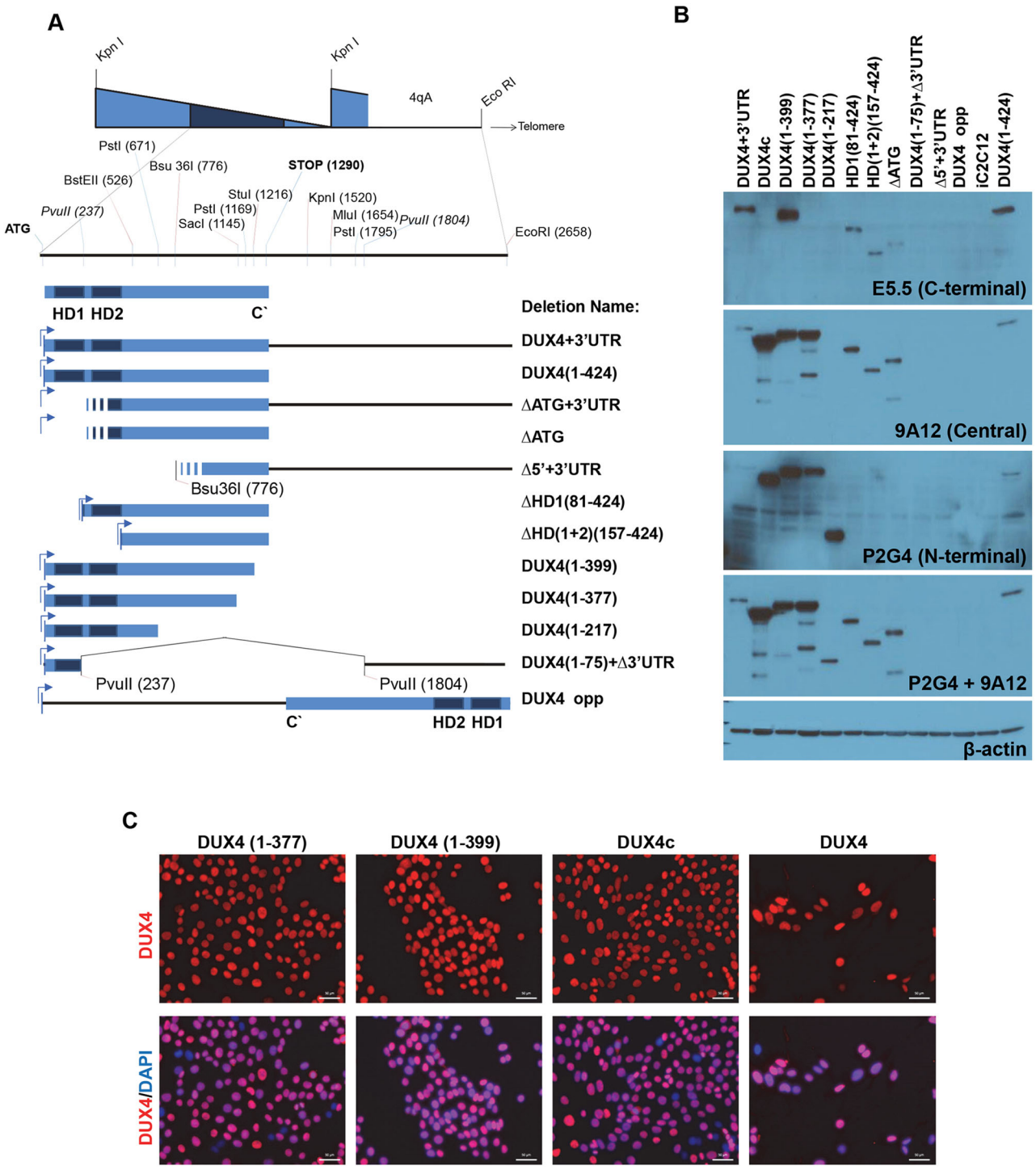

Fig. 1. DUX4 deletion constructs and their inducibility. (A) Diagram of the DUX4 deletion constructs. 2.7 kb of DNA sequence containing the DUX4-ORF from the last full D4Z4 repeat, followed by its 3′UTR, was used as the template to generate deletions. Deletions were named with the amino acids of DUX4, listed as numbers in parentheses. HD denotes homeodomain. 'DUX4' used elsewhere in the manuscript may refer to either DUX4-ORF or DUX4+UTR. Stripes at the 5′ of some constructs indicate an unknown start signal as they lack the DUX4 ATG. (B) Western blotting demonstrates the expression and relative mass of each construct after 12 h of induction with 250 ng ml^{-1} of doxycycline. Protein expression was detected by DUX4-specific antibodies recognizing the N-terminus (P2G4), central (9A12) or C- terminus (E5-5) of DUX4; β-actin levels are also shown. (C) Immunostaining with DUX4 antibody (RD247c) and DAPI (nuclei, blue) of cells induced for 20 h with 250 ng ml^{-1} doxycycline in selected cell lines. Note that almost all of the nuclei are positively stained. Scale bars: 50 µm.

(25 ng ml^{-1}), the shorter constructs were less effective at inhibiting differentiation than the longer constructs (Fig. 3C). Using immunostaining, we confirmed that the cells that failed to differentiate expressed the deletion construct and had decreased MyoD expression (Fig. 3D,E, and data not shown). This analysis clearly shows that the homeodomains of DUX4 are sufficient for repressing MyoD and Myf5 and inhibiting differentiation. The C-terminus leads directly or indirectly to transcriptional activation of

Journal of Cell Science (2017) 130, 3685-3697 doi:10.1242/jcs.205427

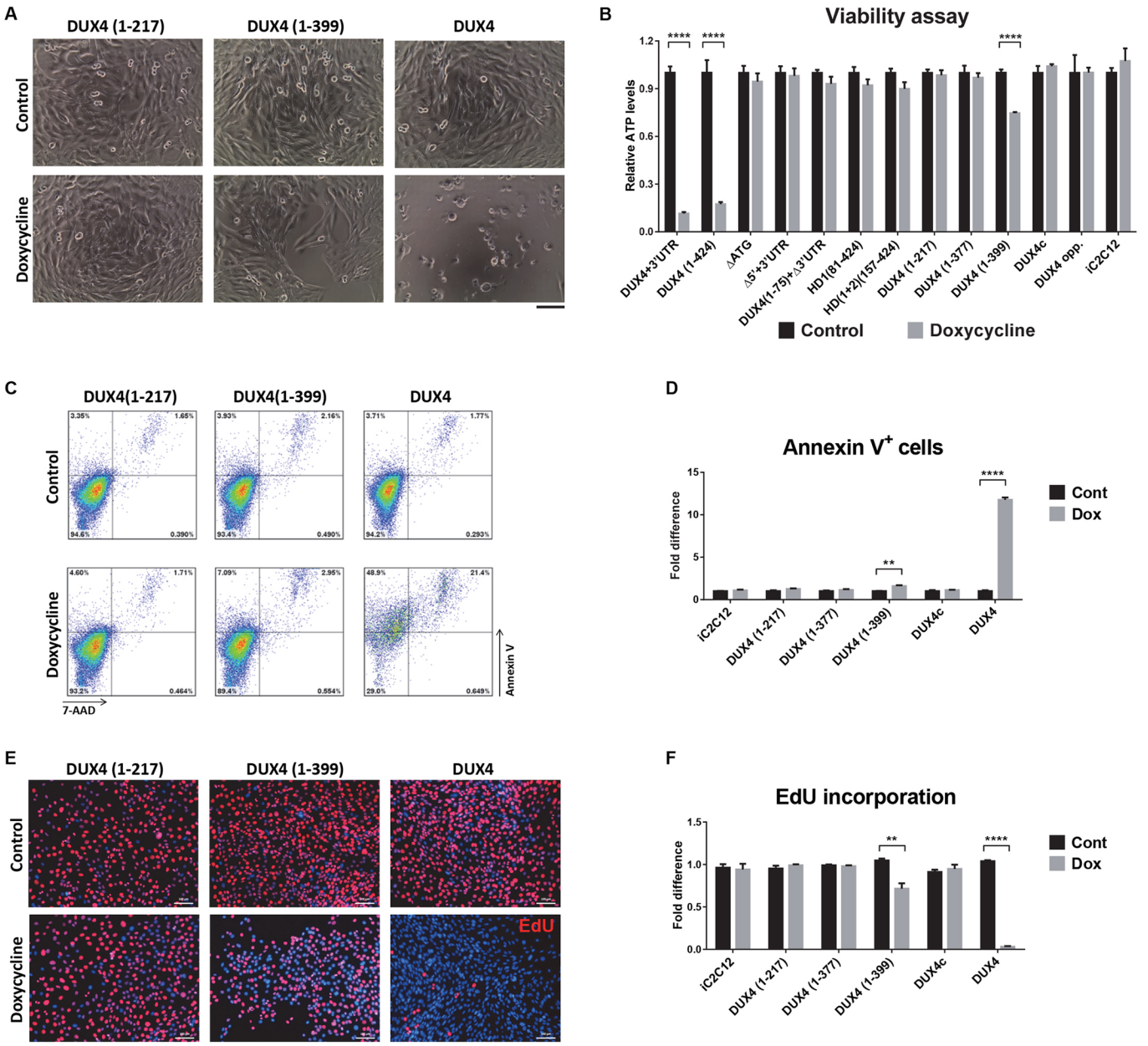

Fig. 2. Effect of DUX4 deletion constructs on cell viability and proliferation. (A) Representative images of cell morphology after 24 h induction with 500 ng ml^{-1} doxycycline. Of all of the tested constructs, only the two encoding an intact full-length DUX4 protein induced rapid cell death. Cells expressing DUX4(1–399) construct were less confluent. (B) ATP assay for quantification of cell viability after 48 h of induction with 500 ng ml^{-1} doxycycline (n=8). (C) Representative FACS analyses of cells induced with 500 ng ml^{-1} doxycycline for 18 h and stained with Annexin V and 7-AAD. (D) Percentage of Annexin V-positive cells in different cell lines after 18 h induction with 500 ng ml^{-1} doxycycline (n=4). (E) Representative images of cells labeled with EdU. Cells were induced for 12 h with 250 ng ml^{-1} doxycycline and labeled for an additional 12 h with EdU. EdU-labeled cells were stained red and nuclei were counterstained with Hoechst 33342 (blue). (F) EdU incorporation in iC2C12 cells induced with various deletion constructs (n=6). All data are presented as fold difference compared with the values for uninduced (control) cells; mean±s.e.m., one-way ANOVA. **P<0.01 ****P<0.0001. Scale bars: 50 µm (E), 100 µm (A).

Myf5 (but not MyoD), which overrides the repression that would be imparted by the homeodomains alone.

MYOD expression restores differentiation

To test whether downregulation of MyoD is one of the reasons for DUX4 inhibition of myogenic differentiation, we overexpressed MYOD in DUX4(1–377) cells using MSCV-MYOD-ires-GFP vector. As a control, we used empty MSCV-ires-GFP. Successful integration of the vectors was monitored by detection of GFP by fluorescence-activated cell sorting (FACS) (Fig. 4A). For this experiment, we used human MYOD to distinguish easily between expression of the transgene and expression of endogenous MyoD (Fig. 4B). Although we detected ectopic expression of human MYOD, endogenous MyoD was still suppressed by DUX4(1–377) at 14 h post induction (Fig. 4B). Restoring MYOD was sufficient to revert the effect of DUX4(1–377) on differentiation. The iC2C12-DUX4(1–377)&MYOD [i.e. inducible DUX4(1–377) and constitutive MYOD expression] cell line induced by a high level of doxycycline (250 ng ml^{-1}) differentiated normally, similarly to the uninduced control cell line (Fig. 4C,D). Thus, we concluded that

Journal of Cell Science (2017) 130, 3685-3697 doi:10.1242/jcs.205427

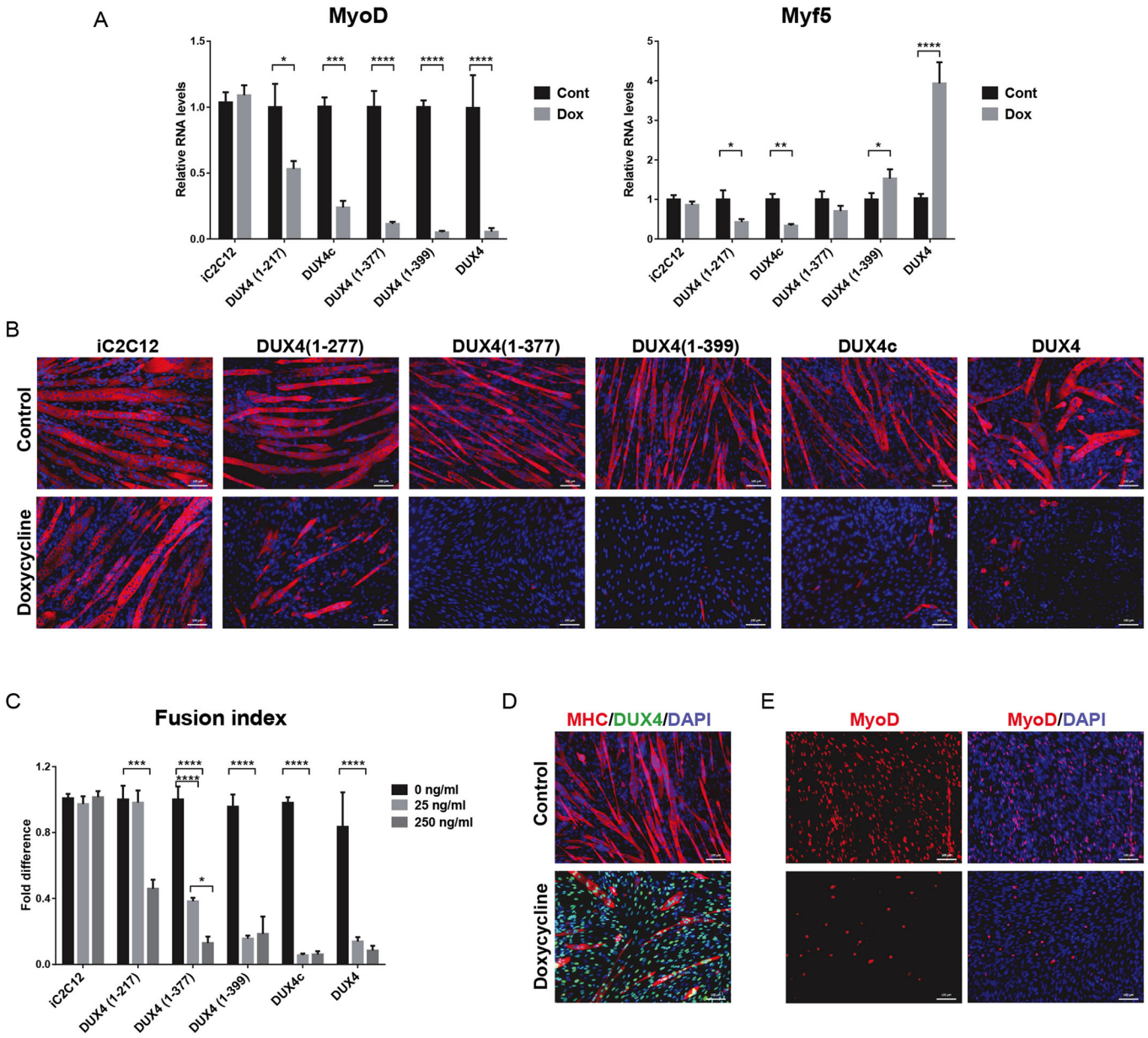

Fig. 3. Effect of DUX4 deletions on myogenesis during proliferation and terminal differentiation. (A) RT-qPCR analyses for *MyoD* and *Myf5* expression in cell lines expressing various deletion constructs induced with 250 ng ml^{-1} doxycycline for 6 h in proliferation medium and compared with uninduced controls (n=4). Gene expression was normalized to the levels of GAPDH. Data are presented as mean±s.e.m., one-way ANOVA. (B) Analysis of myogenic differentiation of the deletion constructs by immunofluorescence for MHC (red). Nuclei were visualized by DAPI staining (blue). Doxycycline (250 ng ml^{-1}) was added for 4 days while cells were cultured in differentiation media. (C) Fusion index analyses for evaluation of levels of myogenic differentiation. Cell lines were differentiated with 25 and 250 ng ml^{-1} doxycycline for 4 days (n=6). Values of induced cells were normalized to the uninduced group. Data are presented as fold difference; mean±s.e.m., two-way ANOVA. (D) Immunostaining for MHC (red), DUX4 (green) and DAPI (blue staining of the nuclei) in iC2C12-DUX4(1–399) at day 4 of differentiation. Cells were induced with 25 ng ml^{-1} doxycycline. Note that all of the cells in the doxycycline-treated group expressed DUX4(1–399). (E) Immunostaining for MyoD (red) and counterstaining of nuclei with DAPI (blue) in iC2C12-DUX4(1–399) at day 4 of differentiation. Note that staining for MyoD is decreased in cells induced with 25 ng ml^{-1} doxycycline. *P<0.05, ***P<0.001, ****P<0.0001. Scale bars: 50 µm in all images.

downregulation of MyoD by DUX4 and DUX4 deletion constructs is one of the reasons for inhibition of myogenesis.

Screening of related homeodomain proteins for suppression of DUX4 toxicity

Previously, we proposed that DUX4 and Pax3/Pax7 might compete for a subset of target genes based on the similarity of their homeodomains (Bosnakovski et al., 2008b). This could impair satellite cells because they express Pax7 when quiescent (Seale et al., 2000) and Pax3 transiently when activated (Conboy and Rando, 2002). In agreement with that hypothesis, we showed that overexpression of the paired-class homeodomain proteins (Pax3 or Pax7), but not the Antennapedia-class homeodomain protein, HoxB4, inhibited DUX4 toxicity. The extent of rescue was dependent on the relative levels of Pax3/Pax7 and DUX4. This competitive interaction is striking, but it is not clear whether it is specific to Pax3 and Pax7, or to the paired class generally. Database searches identified five proteins whose homeodomains are of equal

Journal of Cell Science (2017) 130, 3685-3697 doi:10.1242/jcs.205427

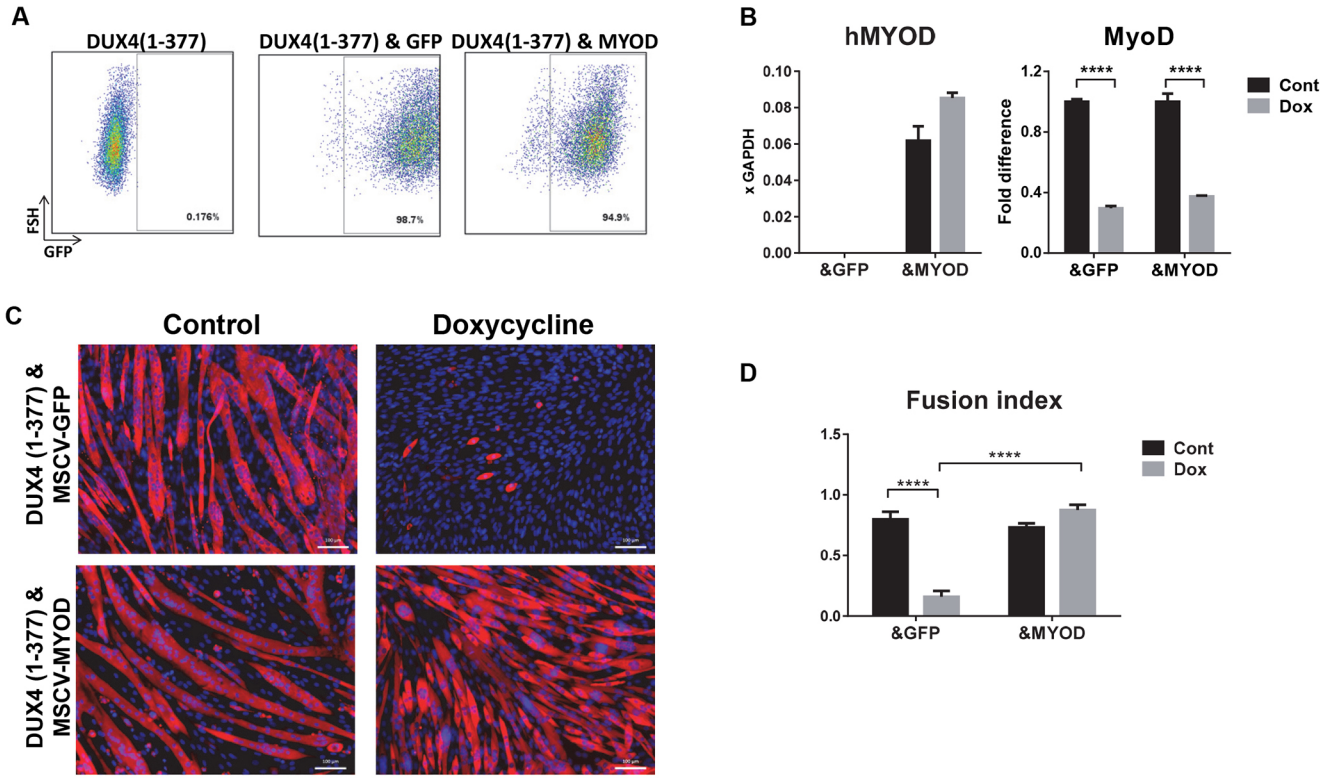

Fig. 4. MYOD overexpression suppresses DUX4-dependent inhibition of differentiation. (A) FACS analyses of iC2C12-DUX4 (1–377) infected with retrovirus carrying GFP or human MYOD-ires-GPP expression vectors. (B) RT-qPCR for human MYOD (MYOD) and endogenous MyoD expression in DUX4 C-terminal deletion, i.e. DUX4(1–377), expressing cell lines transduced with either GFP control (labeled '&GFP') or human MYOD1 (labeled '&MYOD'). Human MYOD1 is shown relative to GAPDH control. Endogenous murine MyoD1 is shown relative to its expression in the absence of Dox. Cells were induced with 250 ng ml^{-1} doxycycline for 14 h (n=4). Data are presented as fold difference compared with control (uninduced cells), mean±s.e.m.; one-way ANOVA. Note that only the DUX4(1–377)&MYOD cell line expressed MYOD. (C) Immunostaining for MHC (red) and DAPI (blue, nuclei) in differentiating cells at day 4 post-induction of differentiation (doxycycline 250 ng ml^{-1}, or control, no dox). Scale bars: 50 µm. (D) Fusion index analysis of the level of differentiation in cells 4 days after differentiation was induced in the presence of 250 ng ml^{-1} doxycycline (n=6). Fusion index represents the ratio of nuclei within myotubes to the total number of nuclei; mean±s.e.m.; two-way ANOVA. ****P<0.0001.

or greater similarity to those of DUX4 compared with Pax3 or Pax7. These proteins are Pax6, Otx1, Rax, Hesx1 and Mixl1 (Fig. 5A,B). We overexpressed each of these genes in iC2C12-DUX4 cells using an MSCV-ires-GFP vector and, by FACS sorting of GFP-positive cells, derived stable homogeneous cell lines expressing the retroviral constructs (Fig. 5C). In addition to testing the set of genes with homeodomains most similar to DUX4, we also analyzed the competitive potential of two other homeobox genes, Tbx1 and Pitx2c, which are known for their involvement in the myogenesis of facial muscle (Sambasivan et al., 2009). The rationale of this approach was that facial muscles are among the muscle groups most affected in FSHD and, consequently, competitive interaction between these two myogenic transcription factors and DUX4 is possible. Because iC2C12 cells can drift phenotypically with passage, this panel of cell lines was generated concurrently and tested immediately; we repeated the generation of Pax3- and Pax7-expressing cells along with the others and an empty vector control. Virus was titred in order to achieve similar transduction rates. Competition was monitored by evaluating cell survival and measuring cell viability (ATP content) in response to a dose-series of DUX4 induction over 48 h. From all tested cell lines, only the cells expressing Pax3 or Pax7 were protected from the acute toxic effect of DUX4 expression. Remarkably, although they contained homeodomains more closely related in sequence, no other proteins were able to competitively inhibit the cytotoxicity of DUX4. This result demonstrates that the competition between DUX4 and Pax3 or Pax7 is not a general feature of highly related paired-class homeodomain proteins.

We next generated a panel of Pax3 deletion mutants to determine which domains were required for effective competition with DUX4 (Fig. 5D). We tested each of these for rescue of DUX4-induced toxicity and found that the octapeptide, paired C-terminal RED domain and aa352–391 within the transactivation domain were dispensible. However, mutants lacking the paired, homeo- or complete transactivation domain were not effective at competing with DUX4 (Fig. 5E). These data clearly show that, although the homeodomain of Pax3 is essential for competition, it is not sufficient.

Toxicity of DUX4-Pax7 homeodomain substitution mutants

To rigorously test whether the homeodomains of DUX4 and the myogenic Pax factors are functionally equivalent, we generated three hybrid proteins in which either the first, second or both DUX4 homeodomains were substituted with the mouse Pax7 homeodomain (Fig. 6A). The Pax3 and Pax7 homeodomains are highly similar, with perfect identity through all DNA-interacting amino acids (Fig. S1). iC2C12 cell lines expressing the hybrid constructs were generated, and inducible protein expression and nuclear localization were confirmed (Fig. 6B,C). We measured toxicity for all three substitution mutant cell lines and WT DUX4 side-by-side. After 48 h of high-level induction, cell death was clearly observed in response to all substitution mutants (Fig. 6D). Immunostaining demonstrated that reduced toxicity in some of the

Journal of Cell Science (2017) 130, 3685-3697 doi:10.1242/jcs.205427

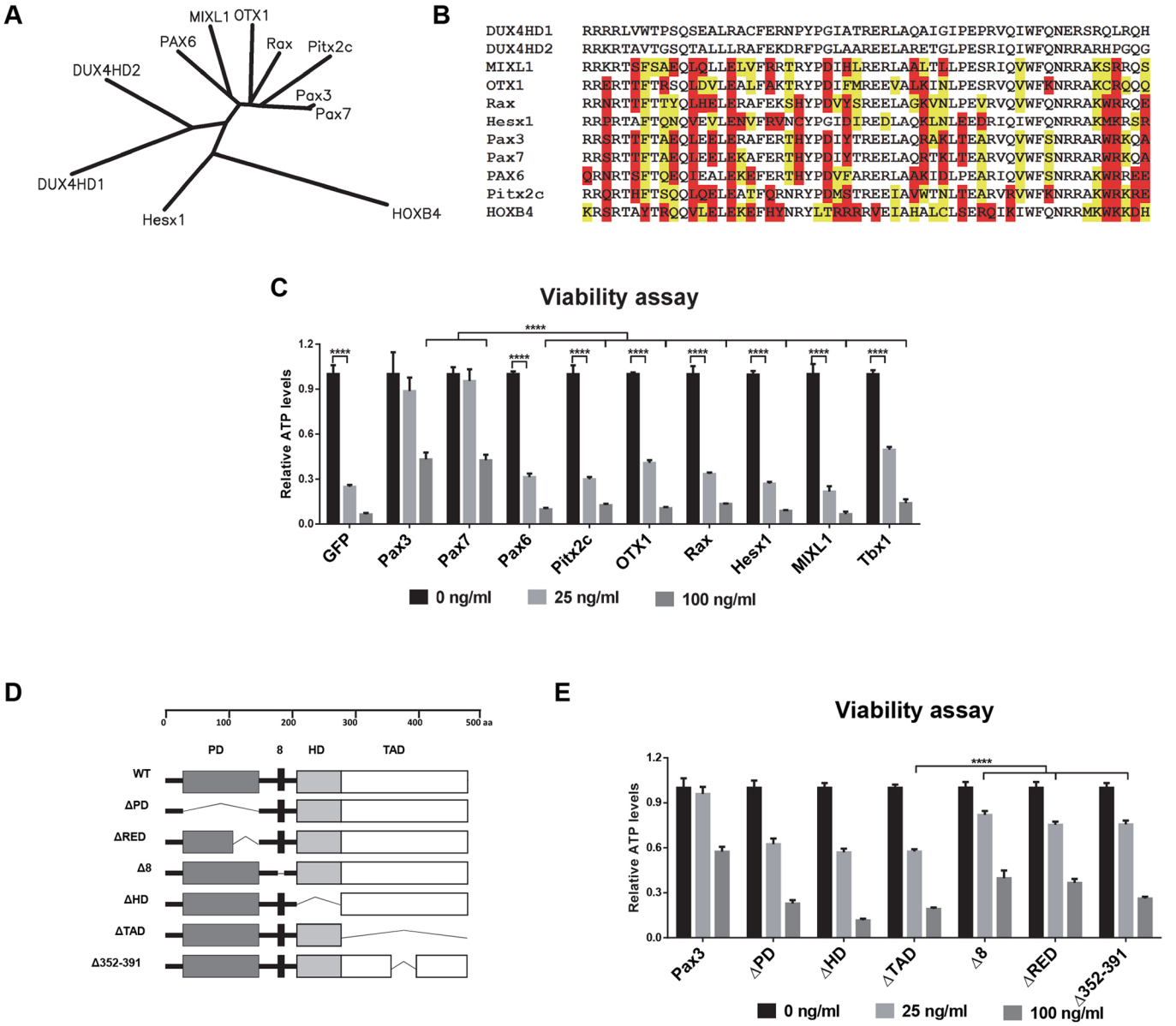

Fig. 5. Assaying homeodomain proteins for dominant suppression of DUX4-induced toxicity. (A) Unrooted dendrogram indicating maximum likelihood sequence relationships between homeodomains of related proteins. (B) Alignment of homeodomain sequences shown in A. Disruptive substitutions (those that change charge, hydrophobicity or conformational freedom) between a given homeodomain and either DUX4HD1 or DUX4HD2 are highlighted in red; conservative substitutions are highlighted in yellow. Sequences are ordered from least to greatest number of disruptive substitutions. Abbreviations for human genes are written in capital letters. (C) Viability assay of induced iC2C12-DUX4 cells constitutively expressing various genes. ATP analyses were done on uninduced cells and cells induced with 25 or 100 ng ml^{-1} doxycycline for 48 h (n=8). Note that of all of the tested candidate genes, only Pax3 and Pax7 were able to act as dominant suppressors by rescuing the DUX4-expressing cells. Values for each doxycycline-induced cell line were normalized to the control uninduced cells. Analyses indicated that all samples were different from their respective controls (i.e. experiencing loss of viability) except Pax3 and Pax7. (D) Diagram of proteins produced from the Pax3 deletion constructs created to map functional domains of the DUX4/Pax3 phenotypic interaction. Domain abbreviations (PD: paired domain; RED: terminal part of the paired domain; 8: octapeptide; HD: homeodomain; TAD: C-terminal activation domain. (E) ATP assay at 48 h post-induction to map Pax3 domains needed for dominant suppression of doxycycline-induced DUX4 lethality (n=8). Each Dox-induced cell line is normalized to control uninduced cells. Note that Pax3, Δ8, ΔRED and Δ352–391 have rescue effects compared with other domain deletion constructs. All data are presented as mean±s.e.m., one-way ANOVA; ****P<0.0001.

cell lines was not caused by non-expressing escapers (Fig. 6C). Measuring viability and apoptosis clearly showed significant cell death in all three homeodomain substitution cell lines, comparable to that observed in iC2C12-DUX4 cells (Fig. 6E–G). In addition, the effects of hybrid proteins with substituted homeodomains on DNA synthesis and cell proliferation were similar to those of WT DUX4, as indicated by EdU incorporation (Fig. 6H), although the HD1+HD2 double substitution showed a weaker effect (Fig. 6I). Thus, we conclude that, regarding effects on viability and apoptosis, the DUX4 and Pax7 homeodomains are in fact functionally interchangeable.

Myogenic effects of DUX4-Pax7 homeodomain substitution mutants

We extended the analysis of homeodomain substitution mutants to myogenic regulatory factor (MRF) expression and myogenesis. When

Journal of Cell Science (2017) 130, 3685-3697 doi:10.1242/jcs.205427

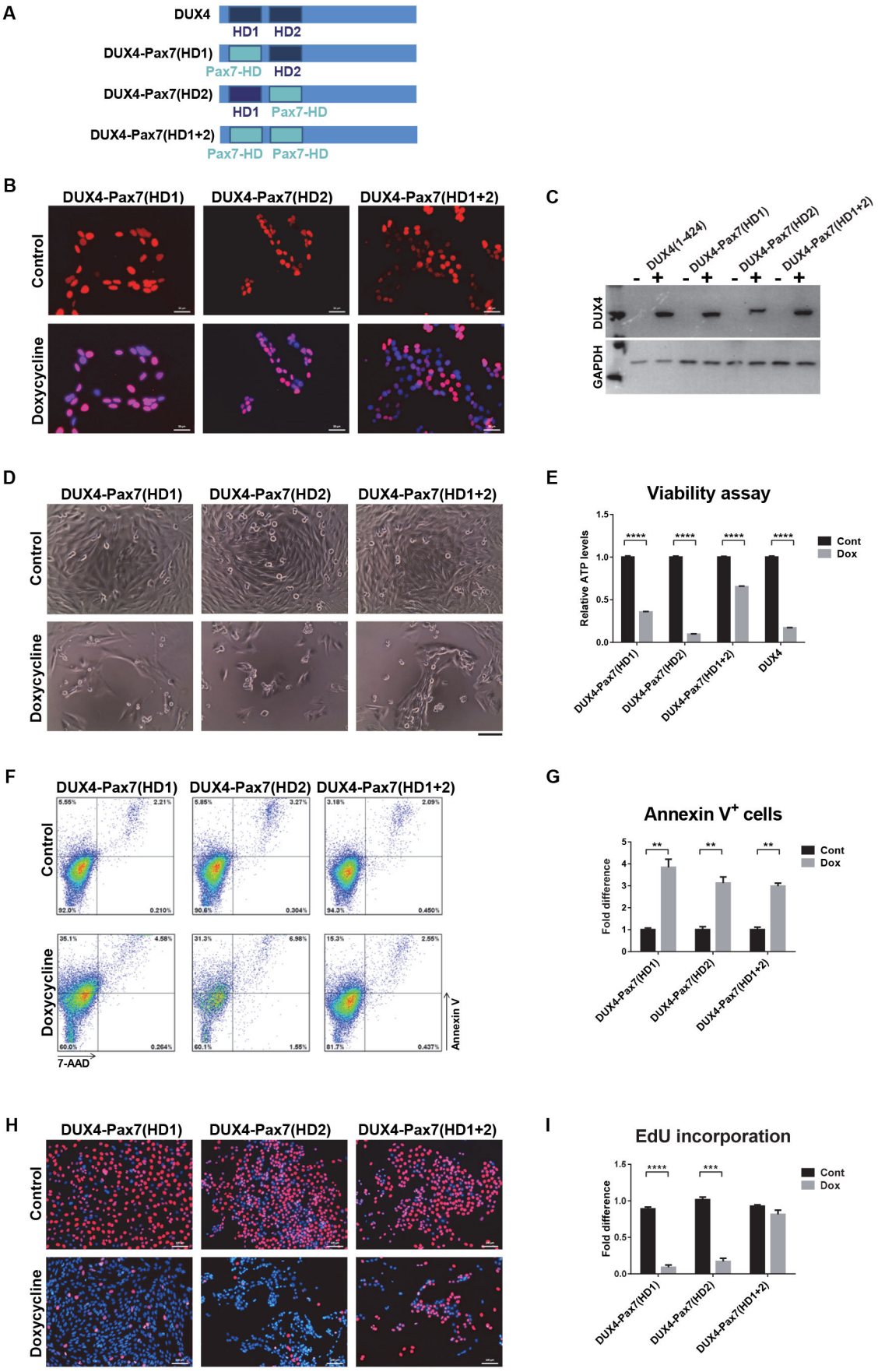

Fig. 6. See next page for legend.

Journal of Cell Science (2017) 130, 3685-3697 doi:10.1242/jcs.205427

Fig. 6. Toxicity of DUX4-Pax7 homeodomain substitutions. (A) DUX4-Pax7 homeodomain substitutions. In the construct DUX4-Pax7(HD1) the first DUX4 homeodomain was substituted, in DUX4-Pax7(HD2) the second, and in DUX4-Pax7(HD1+2) both homeodomains were substituted with the mouse Pax7 homeodomain. (B) Immunostaining revealed nuclear localization of hybrid proteins (red). Cells were induced for 20 h with 250 ng ml^{-1} doxycycline. (C) Western blotting with RD247c antibody shows the protein expression from the hybrid constructs. (D) Cell morphology after 48 h induction with 250 ng ml^{-1} doxycycline. Obvious cell death was observed with induction of all three hybrid constructs. (E) ATP assay for cell viability after 48 h of induction with 500 ng ml^{-1} doxycycline (n=8). (F) FACS analyses of cells induced with 500 ng ml^{-1} doxycycline for 18 h and stained with Annexin V/7-AAD. (G) Percentage of Annexin V-positive cells after 18 h induction with 500 ng ml^{-1} doxycycline (n=4). (H) Representative images of cells labeled with EdU. Cells were induced for 12 h with 250 ng ml^{-1} doxycycline and labeled for an additional 12 h with EdU. EdU-labeled cells are stained with red and nuclei were counterstained with Hoechst 33342 (blue). (I) EdU incorporation in cells presented in H (n=6). All data are presented as fold difference compared with control (uninduced) cells; mean±s.e.m., one-way ANOVA. **P<0.01, ***P<0.001, ****P<0.0001. Scale bars: 50 µm (B,H), 100 µm. (D)

these mutants were cultured under proliferation conditions and induced for 8 h with 250 ng ml^{-1} doxycycline, MyoD RNA levels were decreased significantly in all three hybrid constructs (Fig. 7A). Interestingly, only the construct in which both homeodomains were substituted showed significant upregulation of Myf5 (Fig. 7A). To analyze the effects of the different HD substitution mutants on myogenic differentiation, cells were cultured to confluence, subsequently switched to medium promoting differentiation, and induced with doxycycline at low and high concentrations (25 and 250 ng ml^{-1}) for 4 days. All three hybrid proteins at high levels showed impaired differentiation, as indicated by an absence of distinct myotube formation and by a decreased myotube fusion index (Fig. 7B,C). Notably, hybrid proteins were not as effective as WT DUX4 when induced at low levels (Fig. 7C). The double substitution was weakest, but they all clearly showed a statistically significant inhibition of differentiation comparing no doxycycline to 250 ng ml^{-1} doxycycline. We conclude that the DUX4 homeodomains can be substituted for those of Pax7 to generate a substitution mutant that broadly retains the characteristics of WT DUX4.

DISCUSSION

In this study, we probe the function of various domains of the DUX4 protein by testing a series of deletion and substitution mutants for effects on viability, myogenesis, and gene expression. Importantly, the ICE system used here targets constructs into the same doxycycline-regulated genomic locus (Bosnakovski et al., 2008b). This offers numerous advantages compared to transient gene expression with plasmid DNA or overexpression approaches using integration of viral constructs. Gene expression from a single integration site in a non-silencing locus eliminates variation caused by differences in integration site and copy number. In addition, selection for integration is independent of gene expression. This means that until doxycycline is added, cells are unaffected by the various constructs inserted into their genome, which is an important consideration for toxic genes such as *DUX4*.

Our previous work with DUX4c, which is not toxic (Bosnakovski et al., 2008a), indicated that a domain within the C-terminal 80 amino acids of DUX4 was necessary for toxicity. In the present work, we show that C-terminal mutations increase stability, but decrease activity in most assays. In particular, the DUX4(1–399) deletion highlights the importance of the last 25 amino acids for toxicity. Loss of this region disrupts a weakly conserved sequence motif that defines the DUXC family (Leidenroth and Hewitt, 2010). Humans and rodents have lost the canonical *DUXC* gene, but based on the presence of this C-terminal sequence, *DUX4* is evidently a retrotransposed copy that has subsumed the function of *DUXC* in humans; the *mDux* gene on murine chromosome 10 has done the same in rodents. Interestingly, *DUXC* members *DUX4* and murine *Dux* are also present in tandem repeats (Leidenroth and Hewitt, 2010). The results of our study define several phenotypic features of this C-terminal DUXC signature motif: (1) the presence of this motif predicts toxicity of the DUX protein bearing it, (2) the presence of this motif limits accumulation of the DUX protein, most likely by reducing stability, and (3) this motif is important for activation and suppression of various downstream target genes of DUX4, including MyoD and Myf5.

N-terminal deletions that remove one or both homeodomains result in completely inactive proteins. A previous study supported this finding by showing that a version of DUX4 with five alanine substitutions in HD1 (predicted to abolish the domain) is no longer toxic (Wallace et al., 2011). Whereas the complete DUX4 protein is necessary to induce cell toxicity, the homeodomains alone are sufficient to interfere with myogenesis. These effects could involve changes in MRF expression, most likely MyoD expression, because both full-length and homeodomain-only versions of DUX4 repressed MyoD, but had opposite effects on Myf5. C-terminal deletion studies confirmed that intact DUX4 induces Myf5, but successive deletions of C-terminal sequences cause loss of this induction and a switch to repression. The DUX4(1–377) and DUX4 (1–399) constructs, which are shorter than DUX4 but longer than DUX4c, are on the transition threshold: DUX4(1–399) activates weakly whereas DUX4(1–377) represses weakly. DUX4-mediated induction of Myf5 is unlikely to be an indirect consequence of MyoD diminution, because it was also observed in cells that normally do not express MyoD or Myf5, such as fibroblasts and ES cells (Bosnakovski et al., 2008b).

In addition to *DUX4*, various sense and antisense transcripts, as well as potential siRNA or miRNA fragments originating from D4Z4 but not specific to FSHD, have been described (Snider et al., 2009). A similar bidirectional product found using RT-PCR and RNA-FISH was reported for mouse *Dux* (Clapp et al., 2007). We used several approaches to test whether the transcript originating from D4Z4 had any effect on viability or differentiation separate from the DUX4 ORF. We eliminated the start codon of *DUX4* from the full-length transcript, generated inactive mutants of DUX4 through N-terminal deletions that deleted one or both homeodomains, and placed the whole DUX4 sequence in reverse orientation behind the promoter. Proteins or transcripts were detected from all of these constructs, but none of them exhibited functionality in cell viability, apoptosis, cell cycle or myogenesis assays. When we deleted the ATG and used antibodies that recognized the central and C-terminal parts of DUX4, we detected a protein product, an observation made previously by Snider et al. (2009). Smaller bands on the western blot were not present when the constructs with intact ATG start codons were expressed. This suggests that the DUX4 sequence contains alternative internal initiation sites, which in some situations might be engaged. The functional relevance of these potential alternative transcripts to FSHD remains to be explored, although the small ~40 kDa protein that we observed did not induce an effect on cell viability or interfere with myogenesis. We conclude that the principle deleterious factor within the transcript is the DUX4 ORF.

Because the homeodomains were essential for activity in both toxicity and differentiation assays, and because we had previously shown that Pax3 and Pax7 can act as dominant suppressors of the gene

Journal of Cell Science (2017) 130, 3685-3697 doi:10.1242/jcs.205427

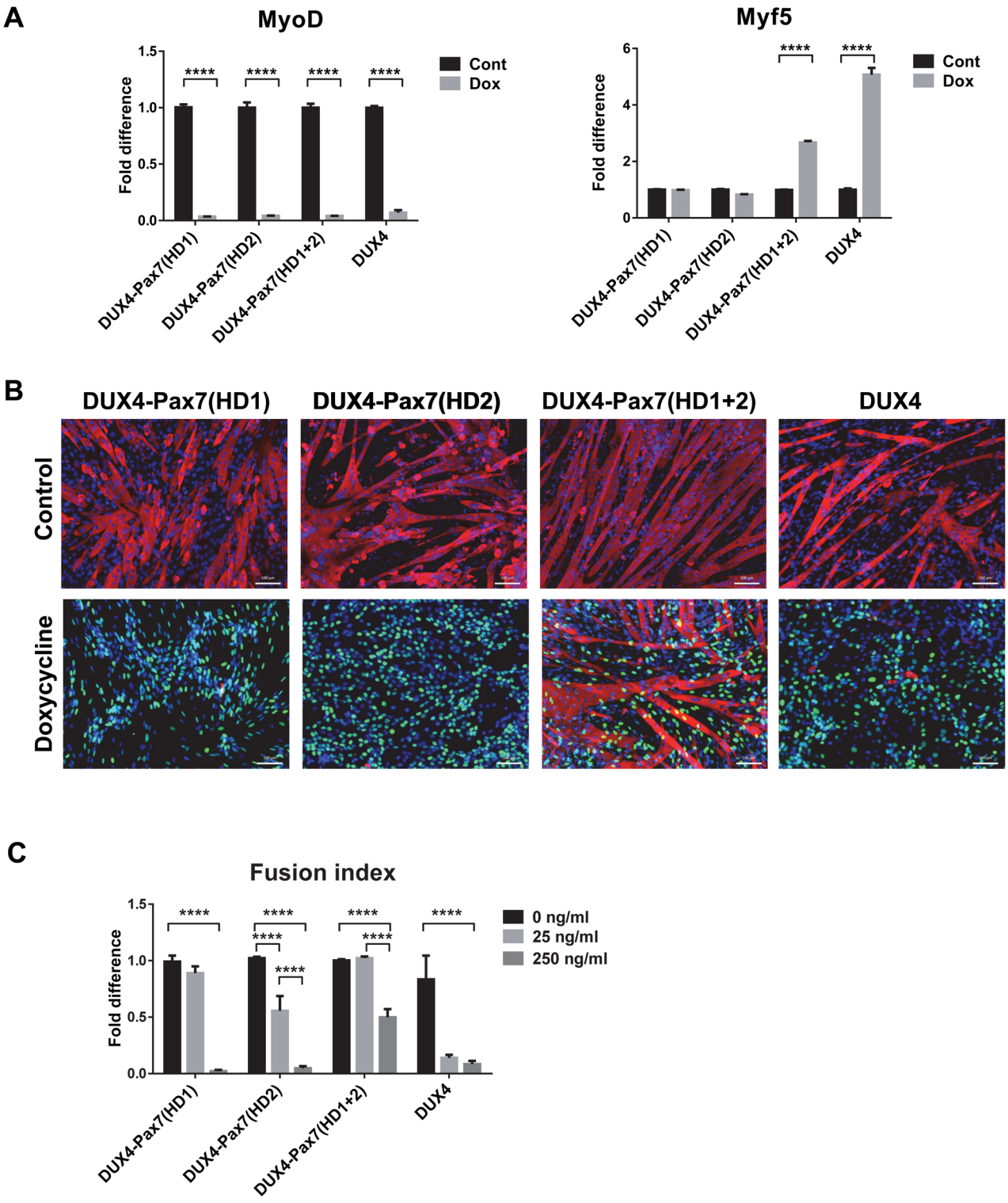

Fig. 7. Effect of homeodomain substitution mutants on myogenesis. (A) RT-qPCR analyses for *MyoD* and *Myf5* expression in the cells induced with 250 ng ml^{-1} doxycycline in proliferation medium for 8 h. Gene expression was normalized to GAPDH expression and presented as fold difference compared with the control samples (n=4). Error bar represents mean±s.e.m., one-way ANOVA. (B) Immunofluorescence for MHC (red), DUX4 (green) and nuclear staining with DAPI (blue) in cells induced with 250 ng ml^{-1} doxycycline for 4 days during myogenic differentiation. (C) Fusion index in cells induced with 25 and 250 ng ml^{-1} doxycycline for 4 days during differentiation (n=6). Data is presented as fold difference of the mean±s.e.m., two-way ANOVA; ***P<0.001 ****P<0.0001.

expression changes and of the toxicity induced by DUX4, we investigated the relationship between DUX4 and these homeodomain-containing proteins in more depth by testing a family of highly related homeodomain-containing proteins. Remarkably, from the set of homeodomain proteins most similar to DUX4, only Pax3 and Pax7 were epistatic to DUX4-induced toxicity. This emphasizes the

Journal of Cell Science

Journal of Cell Science (2017) 130, 3685-3697 doi:10.1242/jcs.205427

specificity of the Pax3/Pax7–DUX4 interaction and its relevance to the myogenic lineage, potentially including the postnatal cells in which Pax3 and Pax7 are expressed. Because of the crucial roles that Pax3 and Pax7 play in embryonic myogenesis and postnatal physiology of the muscle (Bajard et al., 2006; Bober et al., 1994; Braun and Gautel, 2011; Buckingham and Relaix, 2007; Oustanina et al., 2004; Relaix et al., 2005; Seale et al., 2000), this competitive interaction is intriguing. If operative in satellite cells, the presence of DUX4 could interfere with Pax3/Pax7-mediated regenerative regulatory pathways.

In addition, we show that *Pitx2* and *Tbx1*, genes involved in embryonic development of head muscles, are not able to revert DUX4 toxicity. This is also intriguing because facial muscle and the facial muscle satellite cell pool are derived in embryogenesis from Pax3-negative progenitors, whereas limb and body wall muscle are derived from Pax3+ progenitors. Pax3 expression during development might limit the insult caused by low-level DUX4 expression during establishment of the satellite cell pool. If so, the facial muscle founders, which lack Pax3, might be more affected, as is the case in FSHD.

We confirmed the necessity of the Pax3/Pax7 homeodomain for phenotypic competition with DUX4 by deleting it. As expected, Pax3 lacking its homeodomain was not able to compete with DUX4. Unexpectedly however, the paired and activation domains were also found to be necessary. It is unclear whether this means that competition is not at the level of the homeodomain (for example through upregulation of a Pax3/Pax7 target that inhibits the toxic effects of DUX4) or whether the paired and activation domains somehow facilitate direct competition of the Pax3/Pax7 homeodomain with that of DUX4. If the former, one would expect that replacing the DUX4 homeodomains with that of Pax7 would abolish DUX4 toxicity, because the optimal Pax7 and DUX4 DNA recognition sequences are distinct (Geng et al., 2012; Soleimani et al., 2012; Zhang et al., 2016). To evaluate this, we generated hybrid proteins in which the DUX4 homeodomains were substituted with those of Pax7. There were some differences between the constructs, with the double homeodomain substitution being somewhat weaker than each individual substitution. However, all of these hybrid proteins were toxic and inhibited differentiation, like DUX4, showing that the DUX4 and Pax7 homeodomains are functionally interchangeable in spite of having different optimal DNA recognition motifs.

Two possibilities could explain this perplexing result. First, the majority of genomic sites bound by these transcription factors do not have the 'optimal' DNA recognition motif, but variants of it. Although most DUX4 sites are distinct from those of Pax3/Pax7, key toxicity-related targets could have a motif recognized by both DUX4 and Pax3/Pax7. A second possibility is that the homeodomains compete for a homeodomain-interacting protein, rather than for binding to a specific target sequence. Overexpression of Pax3/Pax7 would deplete the DUX4 complex of a key cofactor necessary for full DUX4 activity. Further investigation to address this issue will lead to a better understanding of the toxic activity of DUX4.

MATERIALS AND METHODS

D4Z4 deletion constructs

The terminal D4Z4 repeat (2.7 kb) from pCIneo-DUX4 was used as a template for generating all of the deletion constructs (Gabriëls et al., 1999). To recombine the DUX4 deletion constructs into the ICE locus in iC2C12 myoblasts, they were cloned into p2Lox, the targeting recombination plasmid (Iacovino et al., 2011; Kyba et al., 2002). By directional *XhoI*/*NotI* cloning, a portion of the last D4Z4 repeat was inserted into p2Lox to generate the p2Lox-DUX4+3′UTR construct (Bosnakovski et al., 2008b). The DUX4 ORF [named DUX4(1–424)] construct was generated by PCR using a forward primer (5′-CTCGAGATGGCCCTCCCGAC-3′) to introduce an *XhoI* cutting site and reverse primers at the end of the sequence. ATG deletion constructs were made by PCR by omitting the ATG start codon in the forward amplification primer (5′-CTCGAGGCCCT-CCCGACACC-3′). Deletion of the first, second or both homeodomains was accomplished by PCR with specific forward primers with ATG added to start translation. The Δ5′+3′UTR construct was made by cutting the p2Lox-DUX4+3′UTR plasmid with *XhoI* and *Bsu36I*, and blunt end religation. Additional 3′ deletions of DUX4 were generated by cutting p2Lox-Dux4 with *NotI* and *StuI* for DUX4(1–399), *NotI* and *SacI* for DUX4(1–377), and *NotI* and *PstI* for DUX4(1–217) followed by blunt end religation of the plasmid. ΔDUX4(1–75)+Δ3′UTR was generated by removing the *PvuII* flanked sequence in ΔDux4+3′UTR. For DUX4 opposite (DUX4 opp), the whole D4Z4 sequence was cloned into the opposite orientation in p2Lox. The integrity of each deletion construct was confirmed by sequencing.

Cell culture

iC2C12 cells bearing different deletion constructs were expanded in proliferation medium consisting of high glucose Dulbecco's modified Eagle medium (DMEM) supplemented with L-glutamine, sodium pyruvate, penicillin and streptomycin (P/S; all from Gibco, Invitrogen, Carlsbad, CA) and 10% fetal bovine serum (HyClone, Thermoscientific, Logan, UT) at 37°C in 5% CO_2. Myogenic differentiation was induced in confluent cells cultured on gelatin-coated dishes with DMEM supplemented with 2% horse serum (Sigma, St. Louis, MO) and ITS supplement (Gibco) for 4 days. Cells were authenticated by PCR for the unique ICE locus and by western blot for size of induced proteins, and tested negative for contamination.

Generating iC2C12-DUX4 deletion cell lines

Inducible cell lines with the various constructs were made as previously described (Bosnakovski et al., 2008b). Briefly, iC2C12 myoblasts were induced to express Cre recombinase with 500 ng ml^{-1} doxycycline 1 day before targeting the ICE locus. The recombination plasmid, p2Lox carrying the deletion constructs, was transfected using FUGEN 6 (Roche, Indianapolis, IN). On the following day, selection with 800 µg ml^{-1} G418 was initiated. Within 2 weeks, recombinant G418-resistant clones were generated and tested for inducibility of the constructs. For the deletion constructs, which could be detected by DUX4 antibody, expression of the protein was tested by immunostaining and western blotting (see below). For the constructs for which we did not have suitable antibodies, we used RT-PCR followed by sequencing.

Cloning of retroviral constructs and virus production

MSCV-IRES-GFP retroviral expression plasmids containing the various genes of interest were constructed using the Gateway recombination system (Invitrogen). Human *MIXL1* was amplified from pCR4-TOPO-MIXL1, mouse *Hesx1* from pCR4-TOPO-Hesx1, mouse *Rax* from pCMV-SPORT6-Rax, human *OTX1* from pOTB7-OTX1, mouse *Pitx2* from pYX-Asc-Pitx2, and human *PAX6* from pCMV-SPORT6-PAX6 (all from Open Biosystems, Thermoscientific). Mouse *Pax3* and *Pax7* were generated from previously described pcDNA3.1-Pax3 and pBRIT-Pax7 (McKinnell et al., 2008). Mouse *Tbx1* was amplified from cDNA reverse-transcribed from RNA isolated from the pharyngeal arch of mouse embryos (E9.5); all other genes were amplified from plasmid templates encoding their respective cDNAs. Mouse *Pax3* deletions were constructed as described (Magli et al., 2013). The human MYOD expression construct was as previously described (Bosnakovski et al., 2008a). PCR products were purified using the Promega (Madison, WI) Wizard SV Gel & PCR Clean-Up System, then inserted into the pDONR-221 plasmid using the BP Clonase II enzyme mix (Invitrogen). Clones were sequenced by the Iowa State University DNA Facility to ensure sequence integrity. Correct entry clones were subsequently recombined into the MSCV-IRES-GFP destination vector using the LR Clonase II enzyme mix (Invitrogen). Expression clones were screened for proper gene insertion and sequenced. Large-scale DNA preparations were generated with the Nucleobond Xtra Midi Plus DNA purification kit (Macherey-Nagel, Duren, Germany). Retroviral supernatants were produced in 293 T viral packaging cells. Retroviral constructs were co-transfected with pCL-Eco packaging constructs using FUGENE 6 (Roche). Viral supernatant was collected at

48 h post-transfection. iC2C12-DUX4 cells were infected by spin-infection (2000×***g*** at 33°C for 90 min).

ATP assay

iC2C12 cells carrying DUX4 deletions were plated in a 96-well plate (2000 cells/well). Cells were induced the following day with various doxycycline concentrations for 24 or 48 h. ATP assays were performed following the manufacturer's instructions (Promega) by lysing the cells with 100 ul ATPlite and analyzing the luminescence on a POLARstar Optima Microplate Reader (BMG Labtech, Offenburg, Germany). Data was presented as fold difference compared with the control (uninduced cells) as mean±s.d. (n=8) calculated with Xcel software (Microsoft, Redmond, WA).

Annexin V/7-AAD staining

Cells were cultured in proliferation conditions and induced for 18 h with doxycycline. Cells were trypsinized and stained with Annexin V and 7-AAD using APC Annexin V staining kit (BioLegend) according to the manufacturer's instructions. Stained cells were measured on a FACSARIA II (BD) and analyzed using FlowJo (FlowJo, LLC).

EdU incorporation

Cells were plated at low density (1000 cells/well in a 96-well plate) in proliferating medium. EdU labeling and visualization were carried out using the Click-iT® EdU Imaging Kit (Thermo Fisher Scientific). At 12 h post-induction, cells were treated with EdU (1 µM) for an additional 12 h. At 24 h, cells were fixed with 10% formalin and stained following the manufacturer's instructions. Microscopic fluorescent images of each cell line in the presence and absence of doxycycline were taken with Zen Pro at 10× magnification (six images per cell line). ImageJ was used to calculate the proportion of nuclei with positive EdU staining (Alexa Fluor 555). Images with the Hoechst 33342 channel and Alexa Fluor 555 were loaded into ImageJ separately. Each image was rendered into a 16-bit image and then thresholded for maximum clarity. To calculate the proportion of nuclei with positive EdU staining, the number of nuclei counted in the Alexa Fluor 555 channel image was divided by the number of nuclei counted in the Hoechst 33342 channel image, which represents total nuclei present.

Western blotting

Cells were washed twice with PBS, lysed with RIPA buffer (Santa Cruz Biotechnology, Santa Cruz, CA), mixed with loading buffer (BioRad, Hercules, CA) and boiled for 5 min. Proteins were separated by electrophoresis on 10% PAGE gels. The gels were then transferred to PVDF membranes (BioRad) and blocked in 5% skim milk in TBS-T (Tris-buffered saline containing 0.01% Tween 20) for 1 h at room temperature. Primary antibodies that recognize N-terminal E5-5 (Abcam), central RD247c (R&D Systems) and 9A12 or C-terminal (P2G4) epitopes of DUX4 (Dixit et al., 2007; Geng et al., 2011) were diluted in blocking mixture and blots incubated overnight at 4°C. After washing, secondary anti-mouse/rabbit horseradish peroxidase-conjugated antibodies (1:3000; Santa Cruz Biotechnology) were applied for 1 h at room temperature in blocking mixture. Signal was detected by ECL Plus (GE Healthcare, Piscataway, NJ) with X-ray film exposure.

Immunofluorescence

Cells were fixed with 4% paraformaldehyde for 20 min, permeabilized by 0.3%Triton X-100 for 30 min and blocked by 3% BSA in PBS for 1 h at room temperature. Primary antibodies were incubated in 3% BSA in PBS at 4°C overnight, followed by secondary antibodies at room temperature for 45 min. Nuclei were visualized using 4′,6-diamidino-2-phenylindole (DAPI; Invitrogen). The following antibodies were used: mouse anti-MHC (MF20, 1:20; Developmental Studies Hybridoma Bank), rabbit anti-MyoD (1:200; Santa Cruz Biotechnology), rabbit anti-DUX4 (1:50; R&D Systems), Alexa Fluor 555 goat anti-mouse and Alexa Fluor 555 or 488 goat anti-rabbit (1:500; Invitrogen).

Quantitative real-time RT-PCR

RNA was extracted with Trizol (Invitrogen). cDNA was made using 0.5 µg total RNA with oligo-dT primer and ThermoScript following the manufacturer's instructions (Invitrogen). PCR was performed by using TaqMan Real-Time PCR premixture and premix probes (Myod1 Mm00440387_m1, Myf5 Mm00435125_m1, human MYOD1 Hs00159528_m1) on a 7900 HT real-time PCR System (Applied Biosystems, Carlsbad, CA). Glyceraldehyde phosphate dehydrogenase (GAPDH; Mm99999915_g1) was used as the internal standard. All reactions were performed at least in triplicate. Data were normalized and analyzed by 7900 HT System Software using the ΔΔCT method (Applied Biosystems). Data are presented as mean±s.e.m. calculated with Prism (GraphPad, San Diego, CA) software.

Calculating fusion index with G-Tool

G-Tool, a previously developed open-source algorithm, was used to quantify myogenic differentiation. MHC-stained fluorescent images were analyzed and the average number of nuclei per MHC-positive myotube calculated. Microscopic fluorescent images were taken with Zen Pro at 10× magnification. Merged images containing both the DAPI (nuclei) and the Alexa Fluor 555 (MHC) channels were input into the G-Tool user platform. Images were then processed according to default sensitivity and contrast settings. The G-Tool algorithm was then calibrated to the nuclear size in the image library by manual adjustment of DAPI sensitivity and contrast. Once calibrated, the G-Tool algorithm analyzed all images according to this calibration and calculated the fusion index of each condition and replicate using a published method (Ippolito et al., 2012).

Statistical analyses

All experiments were repeated in at least three biological replicates. The significance of the paired differences was calculated using the Student's t-test or one- or two-way ANOVA with GraphPad; $P<0.05$ was considered statistically significant.

Acknowledgements

We thank the Dr Bob and Jean Smith Foundation for their generous support. We thank Dr Daniel Miller for the suggestion to test related homeodomain proteins Hesx1, etc. We thank L. Geng and S. Tapscott for sharing E5-5 and P2G4 antibodies prior to publication and A. Belayew for the 9A12 antibody. The monoclonal antibody against MHC was obtained from the Developmental Studies Hybridoma Bank, developed under the auspices of the NICHD and maintained by the University of Iowa.

Competing interests

The authors declare no competing or financial interests.

Author contributions

Conceptualization: D.B., M.K.; Methodology: D.B., E.A.T., A.M., M.K.; Formal analysis: D.B., M.K.; Investigation: D.B., E.A.T., L.M.H., H.A.L., E.R.T., A.D.; Resources: A.M., R.C.R.P.; Data curation: L.M.H.; Writing - original draft: M.K.; Writing - review & editing: D.B., L.M.H., M.K.; Visualization: L.M.H.; Supervision: R.C.R.P., M.K.; Project administration: M.K.; Funding acquisition: M.K.

Funding

This work was funded by the National Institute of Arthritis and Musculoskeletal and Skin Diseases (AR055685). D.B. was supported by a Muscular Dystrophy Association Development Grant (MDA 4361), a Marjorie Bronfman Research Fellowship from the FSH Society and by the Children's Cancer Research Fund. Deposited in PMC for release after 12 months.

Supplementary information

Supplementary information available online at
http://jcs.biologists.org/lookup/doi/10.1242/jcs.205427.supplemental

References

Bajard, L., Relaix, F., Lagha, M., Rocancourt, D., Daubas, P. and Buckingham, M. E. (2006). A novel genetic hierarchy functions during hypaxial myogenesis: Pax3 directly activates Myf5 in muscle progenitor cells in the limb. *Genes Dev.* **20**, 2450-2464.

Block, G. J., Narayanan, D., Amell, A. M., Petek, L. M., Davidson, K. C., Bird, T. D., Tawil, R., Moon, R. T. and Miller, D. G. (2013). Wnt/beta-catenin signaling suppresses DUX4 expression and prevents apoptosis of FSHD muscle cells. *Hum. Mol. Genet.* **22**, 4661-4672.

Bober, E., Franz, T., Arnold, H. H., Gruss, P. and Tremblay, P. (1994). Pax-3 is required for the development of limb muscles: a possible role for the migration of dermomyotomal muscle progenitor cells. *Development* **120**, 603-612.

Bosnakovski, D., Lamb, S., Simsek, T., Xu, Z., Belayew, A., Perlingeiro, R. and Kyba, M. (2008a). DUX4c, an FSHD candidate gene, interferes with myogenic regulators and abolishes myoblast differentiation. *Exp. Neurol.* **214**, 87-96.

Bosnakovski, D., Xu, Z., Gang, E. J., Galindo, C. L., Liu, M., Simsek, T., Garner, H. R., Agha-Mohammadi, S., Tassin, A., Coppée, F. et al. (2008b). An isogenetic myoblast expression screen identifies DUX4-mediated FSHD-associated molecular pathologies. *EMBO J.* **27**, 2766-2779.

Braun, T. and Gautel, M. (2011). Transcriptional mechanisms regulating skeletal muscle differentiation, growth and homeostasis. *Nat. Rev. Mol. Cell Biol.* **12**, 349-361.

Buckingham, M. and Relaix, F. (2007). The role of pax genes in the development of tissues and organs: pax3 and pax7 regulate muscle progenitor cell functions. *Annu. Rev. Cell Dev. Biol.* **23**, 645-673.

Buckingham, M., Bajard, L., Chang, T., Daubas, P., Hadchouel, J., Meilhac, S., Montarras, D., Rocancourt, D. and Relaix, F. (2003). The formation of skeletal muscle: from somite to limb. *J. Anat.* **202**, 59-68.

Celegato, B., Capitanio, D., Pescatori, M., Romualdi, C., Pacchioni, B., Cagnin, S., Viganò, A., Colantoni, L., Begum, S., Ricci, E. et al. (2006). Parallel protein and transcript profiles of FSHD patient muscles correlate to the D4Z4 arrangement and reveal a common impairment of slow to fast fibre differentiation and a general deregulation of MyoD-dependent genes. *Proteomics* **6**, 5303-5321.

Choi, S. H., Gearhart, M. D., Cui, Z., Bosnakovski, D., Kim, M., Schennum, N. and Kyba, M. (2016). DUX4 recruits p300/CBP through its C-terminus and induces global H3K27 acetylation changes. *Nucleic Acids Res.* **44**, 5161-5173.

Clapp, J., Mitchell, L. M., Bolland, D. J., Fantes, J., Corcoran, A. E., Scotting, P. J., Armour, J. A. L. and Hewitt, J. E. (2007). Evolutionary conservation of a coding function for D4Z4, the tandem DNA repeat mutated in facioscapulohumeral muscular dystrophy. *Am. J. Hum. Genet.* **81**, 264-279.

Conboy, I. M. and Rando, T. A. (2002). The regulation of Notch signaling controls satellite cell activation and cell fate determination in postnatal myogenesis. *Dev. Cell* **3**, 397-409.

Dixit, M., Ansseau, E., Tassin, A., Winokur, S., Shi, R., Qian, H., Sauvage, S., Matteotti, C., van Acker, A. M., Leo, O. et al. (2007). DUX4, a candidate gene of facioscapulohumeral muscular dystrophy, encodes a transcriptional activator of PITX1. *Proc. Natl. Acad. Sci. USA* **104**, 18157-18162.

Gabellini, D., Green, M. R. and Tupler, R. (2002). Inappropriate gene activation in FSHD: a repressor complex binds a chromosomal repeat deleted in dystrophic muscle. *Cell* **110**, 339-348.

Gabriëls, J., Beckers, M.-C., Ding, H., De Vriese, A., Plaisance, S., van der Maarel, S. M., Padberg, G. W., Frants, R. R., Hewitt, J. E., Collen, D. et al. (1999). Nucleotide sequence of the partially deleted D4Z4 locus in a patient with FSHD identifies a putative gene within each 3.3 kb element. *Gene* **236**, 25-32.

Geng, L. N., Tyler, A. E. and Tapscott, S. J. (2011). Immunodetection of human double homeobox 4. *Hybridoma (Larchmt)* **30**, 125-130.

Geng, L. N., Yao, Z., Snider, L., Fong, A. P., Cech, J. N., Young, J. M., van der Maarel, S. M., Ruzzo, W. L., Gentleman, R. C., Tawil, R. et al. (2012). DUX4 activates germline genes, retroelements, and immune mediators: implications for facioscapulohumeral dystrophy. *Dev. Cell* **22**, 38-51.

Iacovino, M., Bosnakovski, D., Fey, H., Rux, D., Bajwa, G., Mahen, E., Mitanoska, A., Xu, Z. and Kyba, M. (2011). Inducible cassette exchange: a rapid and efficient system enabling conditional gene expression in embryonic stem and primary cells. *Stem Cells* **29**, 1580-1588.

Ippolito, J., Arpke, R. W., Haider, K. T., Zhang, J. and Kyba, M. (2012). Satellite cell heterogeneity revealed by G-Tool, an open algorithm to quantify myogenesis through colony-forming assays. *Skelet Muscle* **2**, 13.

Jones, T. I., Chen, J. C. J., Rahimov, F., Homma, S., Arashiro, P., Beermann, M. L., King, O. D., Miller, J. B., Kunkel, L. M., Emerson, C. P.Jr et al. (2012). Facioscapulohumeral muscular dystrophy family studies of DUX4 expression: evidence for disease modifiers and a quantitative model of pathogenesis. *Hum. Mol. Genet.* **21**, 4419-4430.

Knopp, P., Krom, Y. D., Banerji, C. R. S., Panamarova, M., Moyle, L. A., den Hamer, B., van der Maarel, S. M. and Zammit, P. S. (2016). DUX4 induces a transcriptome more characteristic of a less-differentiated cell state and inhibits myogenesis. *J. Cell Sci.* **129**, 3816-3831.

Kowaljow, V., Marcowycz, A., Ansseau, E., Conde, C. B., Sauvage, S., Mattéotti, C., Arias, C., Corona, E. D., Nuñez, N. G., Leo, O. et al. (2007). The DUX4 gene at the FSHD1A locus encodes a pro-apoptotic protein. *Neuromuscul. Disord.* **17**, 611-623.

Krom, Y. D., Dumonceaux, J., Mamchaoui, K., den Hamer, B., Mariot, V., Negroni, E., Geng, L. N., Martin, N., Tawil, R., Tapscott, S. J. et al. (2012). Generation of isogenic D4Z4 contracted and noncontracted immortal muscle cell clones from a mosaic patient: a cellular model for FSHD. *Am. J. Pathol.* **181**, 1387-1401.

Kyba, M., Perlingeiro, R. C. R. and Daley, G. Q. (2002). HoxB4 confers definitive lymphoid-myeloid engraftment potential on embryonic stem cell and yolk sac hematopoietic progenitors. *Cell* **109**, 29-37.

Leidenroth, A. and Hewitt, J. E. (2010). A family history of DUX4: phylogenetic analysis of DUXA, B, C and Duxbl reveals the ancestral DUX gene. *BMC Evol. Biol.* **10**, 364.

Lemmers, R. J. L. F., Tawil, R., Petek, L. M., Balog, J., Block, G. J., Santen, G. W. E., Amell, A. M., van der Vliet, P. J., Almomani, R., Straasheijm, K. R. et al. (2012). Digenic inheritance of an SMCHD1 mutation and an FSHD-permissive D4Z4 allele causes facioscapulohumeral muscular dystrophy type 2. *Nat. Genet.* **44**, 1370-1374.

Magli, A., Schnettler, E., Rinaldi, F., Bremer, P. and Perlingeiro, R. C. R. (2013). Functional dissection of Pax3 in paraxial mesoderm development and myogenesis. *Stem Cells* **31**, 59-70.

McKinnell, I. W., Ishibashi, J., Le Grand, F., Punch, V. G. J., Addicks, G. C., Greenblatt, J. F., Dilworth, F. J. and Rudnicki, M. A. (2008). Pax7 activates myogenic genes by recruitment of a histone methyltransferase complex. *Nat. Cell Biol.* **10**, 77-84.

Montarras, D., Morgan, J., Collins, C., Relaix, F., Zaffran, S., Cumano, A., Partridge, T. and Buckingham, M. (2005). Direct isolation of satellite cells for skeletal muscle regeneration. *Science* **309**, 2064-2067.

Oustanina, S., Hause, G. and Braun, T. (2004). Pax7 directs postnatal renewal and propagation of myogenic satellite cells but not their specification. *EMBO J.* **23**, 3430-3439.

Rahimov, F., King, O. D., Leung, D. G., Bibat, G. M., Emerson, C. P., Jr, Kunkel, L. M. and Wagner, K. R. (2012). Transcriptional profiling in facioscapulohumeral muscular dystrophy to identify candidate biomarkers. *Proc. Natl. Acad. Sci. USA* **109**, 16234-16239.

Relaix, F., Rocancourt, D., Mansouri, A. and Buckingham, M. (2005). A Pax3/Pax7-dependent population of skeletal muscle progenitor cells. *Nature* **435**, 948-953.

Sambasivan, R., Gayraud-Morel, B., Dumas, G., Cimper, C., Paisant, S., Kelly, R. G. and Tajbakhsh, S. (2009). Distinct regulatory cascades govern extraocular and pharyngeal arch muscle progenitor cell fates. *Dev. Cell* **16**, 810-821.

Seale, P., Sabourin, L. A., Girgis-Gabardo, A., Mansouri, A., Gruss, P. and Rudnicki, M. A. (2000). Pax7 is required for the specification of myogenic satellite cells. *Cell* **102**, 777-786.

Snider, L., Asawachaicharn, A., Tyler, A. E., Geng, L. N., Petek, L. M., Maves, L., Miller, D. G., Lemmers, R. J. L. F., Winokur, S. T., Tawil, R. et al. (2009). RNA transcripts, miRNA-sized fragments and proteins produced from D4Z4 units: new candidates for the pathophysiology of facioscapulohumeral dystrophy. *Hum. Mol. Genet.* **18**, 2414-2430.

Snider, L., Geng, L. N., Lemmers, R. J., Kyba, M., Ware, C. B., Nelson, A. M., Tawil, R., Filippova, G. N., van der Maarel, S. M., Tapscott, S. J. et al. (2010). Facioscapulohumeral dystrophy: incomplete suppression of a retrotransposed gene. *PLoS Genet.* **6**, e1001181.

Soleimani, V. D., Punch, V. G., Kawabe, Y., Jones, A. E., Palidwor, G. A., Porter, C. J., Cross, J. W., Carvajal, J. J., Kockx, C. E. M., van Ijcken, W. F. J. et al. (2012). Transcriptional dominance of pax7 in adult myogenesis is due to high-affinity recognition of homeodomain motifs. *Dev. Cell* **22**, 1208-1220.

Tassin, A., Laoudj-Chenivesse, D., Vanderplanck, C., Barro, M., Charron, S., Ansseau, E., Chen, Y. W., Mercier, J., Coppee, F. and Belayew, A. (2012). DUX4 expression in FSHD muscle cells: how could such a rare protein cause a myopathy? *J. Cell. Mol. Med.* **17**, 76-89.

Tsumagari, K., Chang, S.-C., Lacey, M., Baribault, C., Chittur, S. V., Sowden, J., Tawil, R., Crawford, G. E. and Ehrlich, M. (2011). Gene expression during normal and FSHD myogenesis. *BMC Med. Genomics* **4**, 67.

van Overveld, P. G., Lemmers, R. J. F. L., Sandkuijl, L. A., Enthoven, L., Winokur, S. T., Bakels, F., Padberg, G. W., van Ommen, G.-J. B., Frants, R. R. and van der Maarel, S. M. (2003). Hypomethylation of D4Z4 in 4q-linked and non-4q-linked facioscapulohumeral muscular dystrophy. *Nat. Genet.* **35**, 315-317.

Wallace, L. M., Garwick, S. E., Mei, W., Belayew, A., Coppee, F., Ladner, K. J., Guttridge, D., Yang, J. and Harper, S. Q. (2011). DUX4, a candidate gene for facioscapulohumeral muscular dystrophy, causes p53-dependent myopathy in vivo. *Ann. Neurol.* **69**, 540-552.

Wijmenga, C., Hewitt, J. E., Sandkuijl, L. A., Clark, L. N., Wright, T. J., Dauwerse, H. G., Gruter, A.-M., Hofker, M. H., Moerer, P., Williamson, R. et al. (1992). Chromosome 4q DNA rearrangements associated with facioscapulohumeral muscular dystrophy. *Nat. Genet.* **2**, 26-30.

Winokur, S. T., Barrett, K., Martin, J. H., Forrester, J. R., Simon, M., Tawil, R., Chung, S.-A., Masny, P. S. and Figlewicz, D. A. (2003a). Facioscapulohumeral muscular dystrophy (FSHD) myoblasts demonstrate increased susceptibility to oxidative stress. *Neuromuscul. Disord.* **13**, 322-333.

Winokur, S. T., Chen, Y.-W., Masny, P. S., Martin, J. H., Ehmsen, J. T., Tapscott, S. J., van der Maarel, S. M., Hayashi, Y. and Flanigan, K. M. (2003b). Expression profiling of FSHD muscle supports a defect in specific stages of myogenic differentiation. *Hum. Mol. Genet.* **12**, 2895-2907.

Zhang, Y., Lee, J. K., Toso, E. A., Lee, J. S., Choi, S. H., Slattery, M., Aihara, H. and Kyba, M. (2016). DNA-binding sequence specificity of DUX4. *Skelet Muscle* **6**, 8.